**Article:**

Tapoglou, N., Clulow, J., Patterson, A. et al. (1 more author) (2022) Characterisation of mechanical properties of 15-5PH stainless steel manufactured through direct energy deposition. CIRP Journal of Manufacturing Science and Technology, 38. pp. 172-185. ISSN 1755-5817

https://doi.org/10.1016/j.cirpj.2022.04.004

CIRP Journal of Manufacturing Science and Technology 38 (2022) 172–185

Contents lists available at ScienceDirect

CIRP Journal of Manufacturing Science and Technology

journal homepage: www.elsevier.com/locate/cirpj

# Characterisation of mechanical properties of 15-5PH stainless steel manufactured through direct energy deposition

Nikolaos Tapoglou[a,b,*], Joseph Clulow[a], Andrew Patterson[a], David Curtis[a]

[a] Advanced Manufacturing Research Centre, University of Sheffield, Advanced Manufacturing Park, Wallis Way, Catcliffe, Rotherham S60 5TZ, United Kingdom
[b] Department of Industrial Engineering and Management, International Hellenic University, Thessaloniki Greece

ARTICLE INFO

Available online xxxx

*Keywords:*
Additive manufacturing
Direct energy deposition
Stainless steel
Mechanical testing

ABSTRACT

Manufacturing of components through additive manufacturing has become increasingly popular over the last years. Direct energy deposition (DED) is one of the methods gaining popularity due to the high throughput of the methods compared to powder bed fusion methods. For the establishment of DED as a viable option for manufacturing mission critical components, the material characteristics and the mechanical properties of the deposited material must be thoroughly understood. This research focuses on the investigation of the mechanical properties of 15-5PH stainless steel manufactured with direct energy deposition and the effect of heat treatment on the characteristics of the components that were manufactured. The effect of the orientation of the build relevant to the test orientation was examined with relevant tests while a benchmark against wrought 15-5PH was also examined. Finally, the characteristics of the bond between an AM coupon and a base material were investigated.



## Introduction

As the aerospace market continues to evolve, there is an ever-growing need for new materials and processes that can match the industry's ambition. Two steels that have been getting attention from industry are 15-5PH and 17-7PH, which are martensitic and austenitic precipitation hardened stainless steels respectively [1,2]. 15-5PH is produced by heating to an elevated temperature (1038 °C) to provide solution treatment, followed by air cooling which then produces a martensite microstructure. Finally, the steel is heat treated between 482 and 621 °C to promote the formation and aging of supersaturated precipitates, while still maintaining the martensite matrix [1]. It is however worth noting that retained austenite can be found in some samples after air cooling, and that a small amount of martensite can transform back to austenite during the heat treatment process. When this occurs the austenite tends to form on either retained austenite or at the martensite grain and lath boundaries [3].

The homogeneously distributed precipitates formed are Cu based and around 5–10 nm in diameter, which are fine enough to significantly increase the strength of the steel [3–5]. The precipitates have a core-shell structure, with 80% of the precipitate being pure Cu (core), and the remaining 20% is Ni and Mn that surround the precipitates (shell) [3]. The mechanism for the shell creation is unclear at this point, but is believed to occur during the ageing process.

The net result from the microstructure and precipitates is a high strength steel with acceptable toughness and elongation in the longitudinal and transverse loading direction, while being able to maintain these good mechanical properties up to 315 °C [1]. The wide range of heat treatment options allows the steel to be tailored to match the requirements of the customer, which has contributed to this steel becoming very commercially successful.

The 17-7PH steel has a similar solution-cool-age process to the 15-5PH steel, with the key difference being the higher Ni content which promotes the formation of the semi-austenitic (retained austenite with tempered martensite) microstructure [1,2,6]. It should also be stated that some ferrite can also be present in 17-7PH, which is not found in 15-5PH [1,2]. The aging process plays a vital role for developing this steel, as it simultaneously transforms the microstructure from martensite to semi-austenitic, while also inducing supersaturated precipitation of Cr23C6 carbides [6,7].

Both of these steels follow the traditional vacuum-arc casting and forging route prior to heat treatment, which is ideal for the formation of plates that are often used in the aerospace industry [1]. There is however interest in whether these steels can be successfully produced using additive manufacturing (AM) techniques, with direct

* Corresponding author at: Advanced Manufacturing Research Centre, University of Sheffield, Advanced Manufacturing Park, Wallis Way, Catcliffel, Rotherham S60 5TZ, United Kingdom.
*E-mail addresses:* n.tapoglou@sheffield.ac.uk, ntapoglou@iem.ihu.gr (N. Tapoglou).

https://doi.org/10.1016/j.cirpj.2022.04.004
1755-5817/

energy deposition (DED) being one area that is worth investigating. The key advantages of hybrid DED over the cast and forge route is the greater design freedom from the ability to machine the part midway though deposition and the ability to deposit material on already existing parts, even when there are differences in the composition of the materials [8,9].

Studies into the use of additive 15-5PH have been entirely focused on selective laser melting (SLM) manufacturing. The heating/cooling rates and atmospheric conditions will differ for materials produced by SLM compared to DED, therefore the microstructure and mechanical behaviour of the 15-5PH steel is expected to not be directly comparable.

The microstructure of SLM 15-5 PH after different heat treatments procedures was investigated by Coffy [10]. The heat treatment settings were designed to match the conventionally used settings for cast 15-5PH. They found the microstructure of the SLM samples was always finer than the cast material, with there being regions of equiaxed and elongated columnar grains. The SLM 15-5PH microstructure was almost entirely martensite with small traces of austenite, unlike the cast samples they studied which had no austenite. This microstructure has been verified by other researchers [11].

The thermal history of the deposited material has a significant impact on the microstructure, such as morphology and grain size for the DED processes [12,13]. This is due to the increased heating and cooling rates, the presence of significant thermal gradients, and bulk temperature increment. The solidification rate of the melt pool, the thermal gradient at the interface solid–liquid and the ratio between the cooling rate and the gradient of temperature define the microstructure of a deposited part after solidification [14]. As with most layer metal deposition (LMD) of metals, elongation of grains is present [15] due to the lower initial temperature of the previously deposited layer which results in a higher temperature gradient, higher solidification rates and a more unidirectional heat flux. It can also be found in many cases that the colony growth direction is inherited from previously deposited grains, having the same crystallographic orientation. This indicates that the crystallographic relationship between layers influences the crystallisation process in the blown powder DED process [12,13,16].

This largely uniform directional growth of grain structures is why it's important to investigate the mechanical properties of DED material relative to the sample orientation. It has been found that the elongation properties are greatly affected by this orientation [17]. However, other important factors such as cooling rate are crucial in AM materials [5]. It has been shown that the large thermal mass of the base plate provides cooling through conduction to the lower layers of deposited materials, while the upper layers have a decreased cooling rate. This is particularly the case for thin wall and tower like structures, resulting in a reduction in yield and tensile strengths in these locations in comparison to initial layers [17].

The tensile strength of blown powder DED material is generally 5–20% lower than materials created using forging or hot rolling [17,18]. One reason for this could be the slight increase in porosity of the parts in comparison to forged or hot rolled materials, these micro-voids can support crack growth and propagation [19].

Overall, tensile properties of SLM 15-5PH have been found to be comparable with the wrought version, except for the fatigue which is in the region of 20% lower due to the rough SLM surface that promotes crack initiation [11,20]. As with DED materials the strength of the steel varies with the build orientation [21], with it being found that the ultimate tensile strength and fracture strain reduces with increasing build angle (horizontal to vertical build), however the 0.2% proof stress and Young's Modulus is not affected by build orientation [22]. The decrease in mechanical properties for vertical builds is due to more defects being present in the build layers, which can be more easily propagated during tensile testing [22]. This behaviour is not exclusive to SLM 15-5PH and can also be found in other materials such as Ti-6Al-4V [23].

Studies into SLM 15-5PH precipitation has not been established, therefore it is not known whether precipitation occurs during the build process or the nature of the precipitates after heat treatment. This makes it difficult to estimate the effect of heat treatment on DED 15-5PH without experimental investigation.

Blown powder DED steel in the as built condition typically has high strength characteristics and low plasticity [24]. Heat treatment of 316 L stainless steel was found to reduce the yield strength by approximately 17%, while facilitating a 26% increase in elongation to failure [12]. It was reported that the main reason for a decrease in strength was an increase in grain size caused by the heat treatment.

The aim of this paper is to investigate the mechanical properties of DED 15-5PH that has undergone different post processing techniques, with forged 15-5PH being used as a reference. As there has been no studies on this material, this paper should help determine its viability when compared against SLM and wrought 15-5PH [25]. In addition, the effect of depositing 15-5PH on forged 17-7PH will also be investigated and compared against standard 17-7PH. Should the 15-5/17-7 deposition be successful, it would make it possible to create parts where the material property transition is smoother and reduce the likelihood of mechanical failure at the joint region [26]. This research targets to provide a clear understanding of the properties of DED 15-5PH and show the most ideal processing route for manufacturing this material. The reminder of the research is structured as follows. *Experimental procedure* presents the experimental approach followed in the research. *Experimental method* presents the methods employed in the research with *Results and discussion* presenting the results of the research finally *Conclusion* presents the concluding remarks.

## Experimental procedure

In order to understand fully the microstructural and mechanical behaviour of DED 15-5PH steel, samples were created using different conditions of supply that are realistic to industry. The experimental trials were split in two parts. In the first part the strength of additively manufactured 15-5PH in different heat treatments was compared against a traditional condition of supply and for the purpose of this work will be denoted as "type 1″ coupons. In this phase the conditions of the 15-5PH material tested included 15-5PH in the cast and forged (as a reference), hot isostatic pressing (HIP), heat treated (HT), HIP plus heat treated and as-built conditions with coupons examined both in the longitudinal and transverse direction. The second phase of the investigation focused on a hybrid coupon design in which the 15-5PH material was deposited onto a 17-7PH material block in the cast and forged condition, denoted "type 2″ coupons. Thus, creating a series of coupons that composed of 50% 15-5PH and 50% 17-7PH (15-5PH deposited onto 17-7 PH) in the as built or heat-treated condition. The bond line between the two materials was placed in the middle of the coupon with the bond line perpendicular to the test direction. All of the 17-7PH steel was in the "Condition A state", which involves heating to 1066 °C, followed by the forging operations [2]. In this condition, no supersaturated precipitation has taken place, resulting in the 17-7PH steel having a low strength and high ductility.

In order to ensure that the coupons manufactured and tested were identical, a phased investigation was adopted in the manufacturing, testing and analysis steps.

- Starting from the feedstock material, the powder used was examined with a set of powder analysis techniques to ensure no deviations from the nominal specification of the powder. All parts manufactured derived from the same batch of powder in order to avoid shifts in the particle distribution.

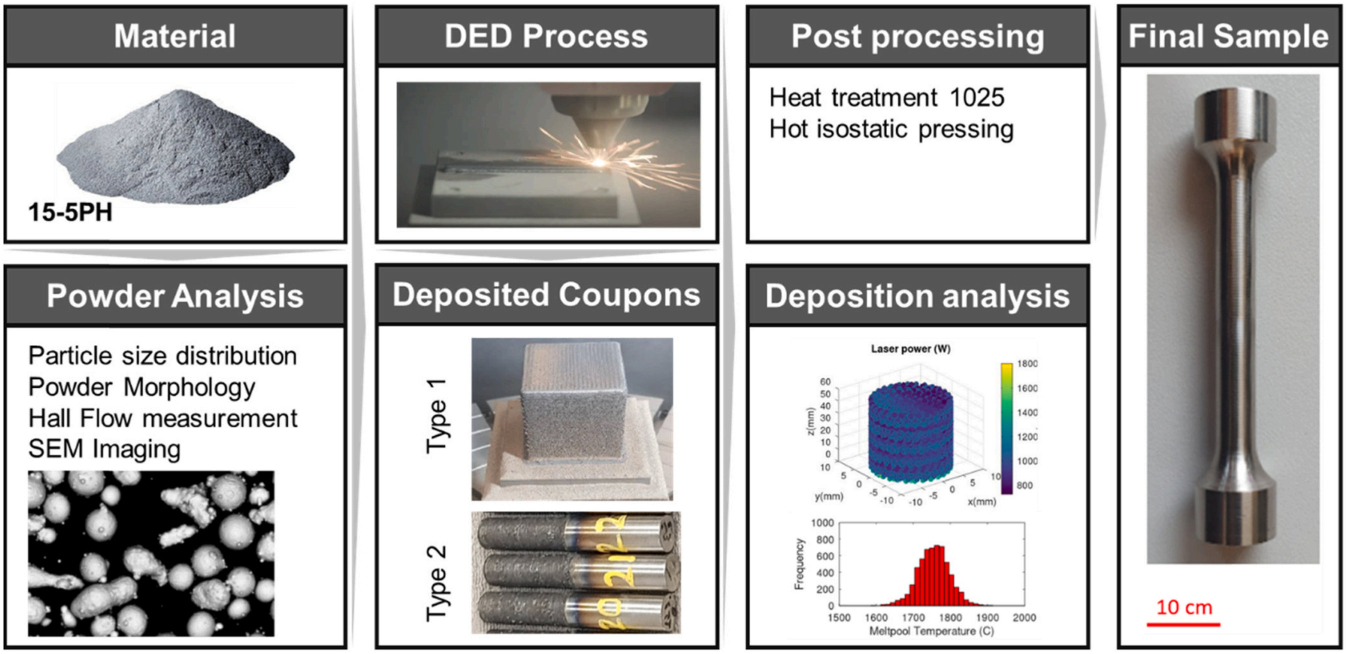


**Fig. 1.** Experimental approach of the testing of DED 15-5PH steel.

- The deposition process was monitored using an onboard monitoring system on the DED platform used. The coupons were manufactured using the same parameters and deposition code without any interruptions that would influence the resulting microstructure.
- After the deposition process the results of the monitoring system were analysed in order to ensure no statistically significant deviations were present between the different coupons.

Fig. 1 summarises the approach followed in the research.

## Experimental method

### *Material*

The material used for the trials consisted of stainless steel 15-5PH in powder form suitable for DED processing. Table 1 gives the chemical composition of the 15-5PH powder used for all of the trials as stated by the supplier in the delivery documentation. It is stated that the powder has a D10, D50, and D90 of 54.2, 75.0 and 104.2 µm respectively and the morphology can be categorised as highly spherical.

**Table 1**
Composition of the 15-5PH DED powder.

| Element | Composition (wt%) |
|---|---|
| C | 0.03 |
| Cr | 14.66 |
| Cu | 3.30 |
| Fe | 76.00 |
| Mn | 0.49 |
| Mo | < 0.1 |
| Nb | 0.28 |
| Ni | 4.52 |
| P | 0.013 |
| S | < 0.010 |
| Si | 0.5 |
| O | 0.022 |
| N | < 0.1 |

The powder was analysed comparing the as delivered, virgin powder with the same powder after a baking operation, aimed at removing any moisture absorbed during transport.

### *Equipment*

The deposition trials were performed on a DMG Mori Lasertec 65 3D Hybrid Ultrasonic machining centre. The machining platform integrates additive manufacturing deposited by blown powder into a 5-axis machining centre, combining the flexibility of the laser metal deposition process with high precision cutting capabilities. The system uses a coaxial powder nozzle to deliver the powder and the shielding gas in the welding zone. The meltpool size and temperature are monitored with the use of a coaxial monochrome camera system that is recording the values every 100 ms. The camera was calibrated by the equipment manufacturer. Throughout the trials, the parameters used were kept constant, except the laser power which was altered with the aim of maintaining a stable melt pool temperature and size. The setup of the machine is presented in Fig. 2.

**Fig. 2.** Experimental setup for the DED deposition trials.

**Table 2**
Deposition parameters.

| | Value | Units |
|---|---|---|
| Laser power | 1800 | W |
| Powder flow rate | 14 | g/min |
| Deposition height | 1.22 | mm |
| Step-over | 1.34 | mm |
| Table Feed | 1000 | mm/min |

All of the additive 15-5PH material was deposited with the parameters outlined in Table 2. The laser power was decreased by 200 W per deposited layer until the laser power was 1000 W, where it was held constant until the build was complete. The parameters on Table 2 were optimised for the specific powder distributions running a process that was also followed in Tapoglou and Clulow [16]. The Type 1 15-5PH coupons were 65 × 65 × 70 mm and were deposited onto a mild steel base plate. From these coupons 14.5 × 14.5 × 60 mm tensile samples were taken using wire electrical discharge machining. Lastly, for the Type 2 hybrid coupons, a forged 17-7PH test piece was used to deposit 15-5PH on top of the coupon with the same X/Y dimensions and height of 102 mm. The deposition time was 194 and 24 min respectively. Specimens were machined and tested to ASTM E8 standard, with specimen size 3 being used [27].

*Deposition analysis*

The deposition parameters monitored during the deposition were further analysed with the use of a custom-built code. The values were extracted from the controller and key information about the meltpool size and temperature were analysed in order to understand the variability between the deposition of successive coupons. The data are presented in the form of spartial maps and intensity histograms.

*Post processing*

Following deposition the parts underwent heat treatment and/or HIP treatment. The heat treatment cycle used was based the H1025 settings, which involved heating to 1025 °F (551 °C), holding for 4 h and air-cooling. HIP was carried out on selected 15-5PH AM blocks prior to machining into tensile coupons. HIP is a process used to reduce porosity of metals, therefore improving the mechanical properties and workability. It functions by subjecting components to high isostatic pressure and temperature and is a technique commonly used to process cast parts and metal powders (Fig. 3).

The parameters used to process the 15-5PH AM materials were as follows:

- Temperature ramp up of 10 °C/min to 1120 °C
- Held at a pressure of 105 MPa and temperature of 1120 °C for 3 h
- Temperature reduced at 50 °C/min

The testing that was carried out is as follows: six type 1 samples in each condition of as-built, HIP, HT, HIP + HT and forged 15-5PH underwent tensile testing with three samples in each category taken from the material in the longitudinal direction and three in the transverse direction. Fig. 4 shows the orientation for these notations with respect to build pattern for type 1 coupons. Three samples from the forged 15-5PH and 17-7PH material, along with the type 2 as-built and HT 50% 15-5/ 50% 17-7 were all tensile tested in the transverse direction. Table 3 presents a summary of the coupons tested.

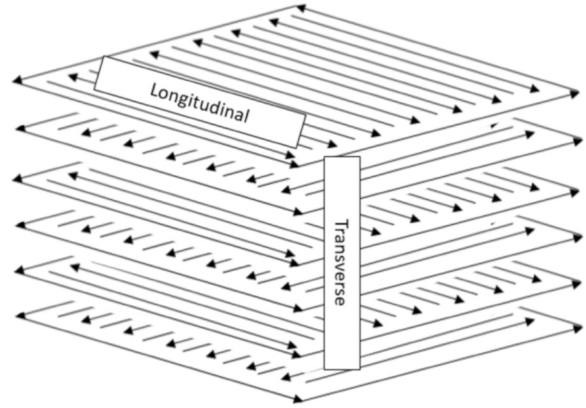


**Fig. 3.** Sample orientation with respect to build pattern for type 1 coupons.

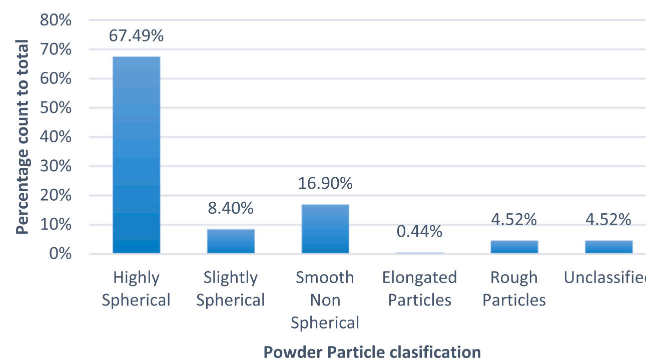


**Fig. 4.** Classification chart for 15-5PH, Baked (number basis).

## Results and discussion

*Powder analysis*

Prior to use the powder was baked to ensure the removal of any moisture absorbed during delivery or storage. The particle size distribution (psd) was measured using laser diffraction technique (Mastersizer 3000). Table 4 shows the results which found no noticeable difference in the psd before and after baking and comparable results to that stated by the manufacturer.

The Morphologi G3 was used in order to provide quantitative morphological data of the powder. This was achieved by taking images of the powder finely spread on a glass slide. The sample consists of thousands of particles and provides information in relation to the shape by categorising the particles into the following morphological classes:

- Highly spherical – particles which have a high degree of circularity as well as smooth surface.
- Slightly spherical – particles which have a relatively smooth surface though also contain some small satellites which are attached to the surface.
- Smooth non spherical – particles which are smooth though are not spherical and contain some satellites.
- Elongated – particles which are far from spherical and exhibit a more elongated shape.
- Rough – particles which have a rough surface due to several satellites and being irregularly shaped.

Fig. 4 shows the percentage of each type of particle for one of the baked powder samples, with the vast majority of particles found to

**Table 3**
Tensile coupons testing summary.

| Coupon type | Material | Heat treatment | Orientation |
|---|---|---|---|
| Type 1 | AM 15-5 PH | As built | Longitudinal, Transverse |
| Type 1 | AM 15-5 PH | HIP | Longitudinal, Transverse |
| Type 1 | AM 15-5 PH | H1025 | Longitudinal, Transverse |
| Type 1 | AM 15-5 PH | HIP+H1025 | Longitudinal, Transverse |
| Type 1 | 15-5 PH | As received | Transverse |
| Type 1 | 17-7 PH | As received | Transverse |
| Type 2 | 50% AM 15-5, 50%17-7 | As built | Transverse |
| Type 2 | 50% AM 15-5, 50%17-7 | H1025 | Transverse |

**Table 4**
Particle size distribution of 15-5PH from the Mastersizer 3000 (error ± standard deviation).

| Sample | $D_{10}$ (μm) | $D_{50}$ (μm) | $D_{90}$ (μm) |
|---|---|---|---|
| 15-5PH_B1_PreBaked | 54.2 ± 0.15 | 75.4 ± 0.30 | 105.3 ± 0.57 |
| 15-5PH_B2_PreBaked | 54.0 ± 0.31 | 74.7 ± 0.25 | 103.7 ± 0.57 |
| 15-5PH_B1_Baked | 54.5 ± 0.03 | 75.4 ± 0.04 | 104.3 ± 0.06 |
| 15-5PH_B2_Baked | 53.9 ± 0.15 | 74.5 ± 0.10 | 103.3 ± 0.58 |
| Manufacturer value | 54.2 | 75.0 | 104.2 |

be highly spherical. Similar results were also found for the other baked samples and non-baked samples.

The Hall Flow (ASTM B213, Method 1) was used to determine the flow rate of the powder as it passed through the Hall flowmeter funnel. A fixed mass (50 g) of powder was timed as it passed through a calibrated orifice (2.54 mm diameter). The flow rate is reported in seconds per 50 g in Table 5.

SEM Images for both the prebaked and baked samples can be seen in Fig. 5 and Fig. 6, respectively. The images show a large presence of smooth particles as well as fines, which agree with the findings from the G3 imaging. The presence of elongated particles can be seen in the magnified images.

The Freeman FT4 powder rheometer, a universal powder tester, was used to measure the dynamic flow, shear and bulk characteristics of the powder and the rheological properties of the powder can be seen in Table 6.

**Table 5**
Hall flow test for 15-5PH (3 runs, error ± standard deviation).

| Batch | Sample | Hall Flow (s/50 g) |
|---|---|---|
| 1 | 15-5PH_PreBaked | 18.5 ± 0.3 |
| 1 | 15-5PH_Baked | 16.6 ± 0.3 |
| 2 | 15-5PH_PreBaked | 16.7 ± 0.1 |
| 2 | 15-5PH_Baked | 16.5 ± 0.1 |
| – | Manufacturer value | 16 |

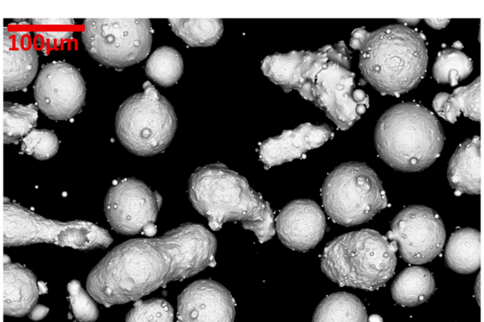


**Fig. 5.** SEM Morphological images for Prebaked 15-5PH.

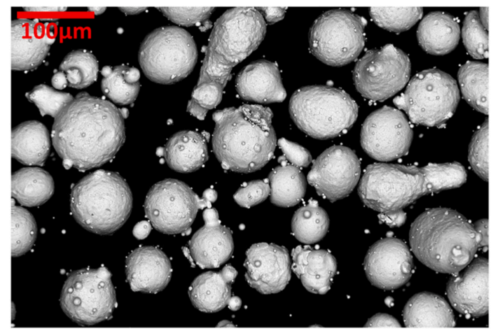


**Fig. 6.** SEM Morphological images for Baked 15-5PH.

- The Basic Flowability Energy (BFE) for both prebaked and baked are similar, though the baked samples for both Batch 1 and 2 were slightly higher.
- The Specific Energy (SE) is similar and less than 5 mJ/g, indicating a low level of cohesion.
- The Flow Rate Index (FRI) shows that in both prebaked and baked states the powder is generally insensitive to the flow rate, which is expected for a non-cohesive powder.
- The Condition Bulk Density (CBD) is similar for all samples indicating that baking does not affect the packing arrangement of the powder.

*Deposition analysis*

Prior to performing the experimental campaign, data acquired from the deposition process were analysed in order to understand the variability between the different samples. During deposition, the melt pool size and temperature as well as the laser power were monitored in regular intervals. Type 1 samples had a more stable geometry, owing to the large size of the deposited structure. Because of the size of the samples, a stable deposition process could be easily achieved and the variability between the components that underwent different regimes of heat treatment was minimal. For the type 2 samples, the relatively small volume of material deposited and the geometry of the sample made them susceptible to instabilities in the deposition process that lead to defects in the final samples thus biasing the results. In order to ensure that there were no faults during the build process that could be detrimental to the results, the in-process characteristics of the deposition process were analysed in

**Table 6**
FT4 rheological properties for 15-5PH (Prebaked and Baked).

| Batch | Sample | BFE (mJ) | FRI | SE (mJ/g) | CBD (g/ml) |
|---|---|---|---|---|---|
| 1 | 15-5PH_PreBaked | 505 | 1.12 | 1.99 | 4.28 |
| 1 | 15-5PH_Baked | 523 | 1.09 | 2.16 | 4.32 |
| 2 | 15-5PH_PreBaked | 541 | 1.15 | 2.27 | 4.27 |
| 2 | 15-5PH_Baked | 537 | 1.11 | 2.20 | 4.31 |

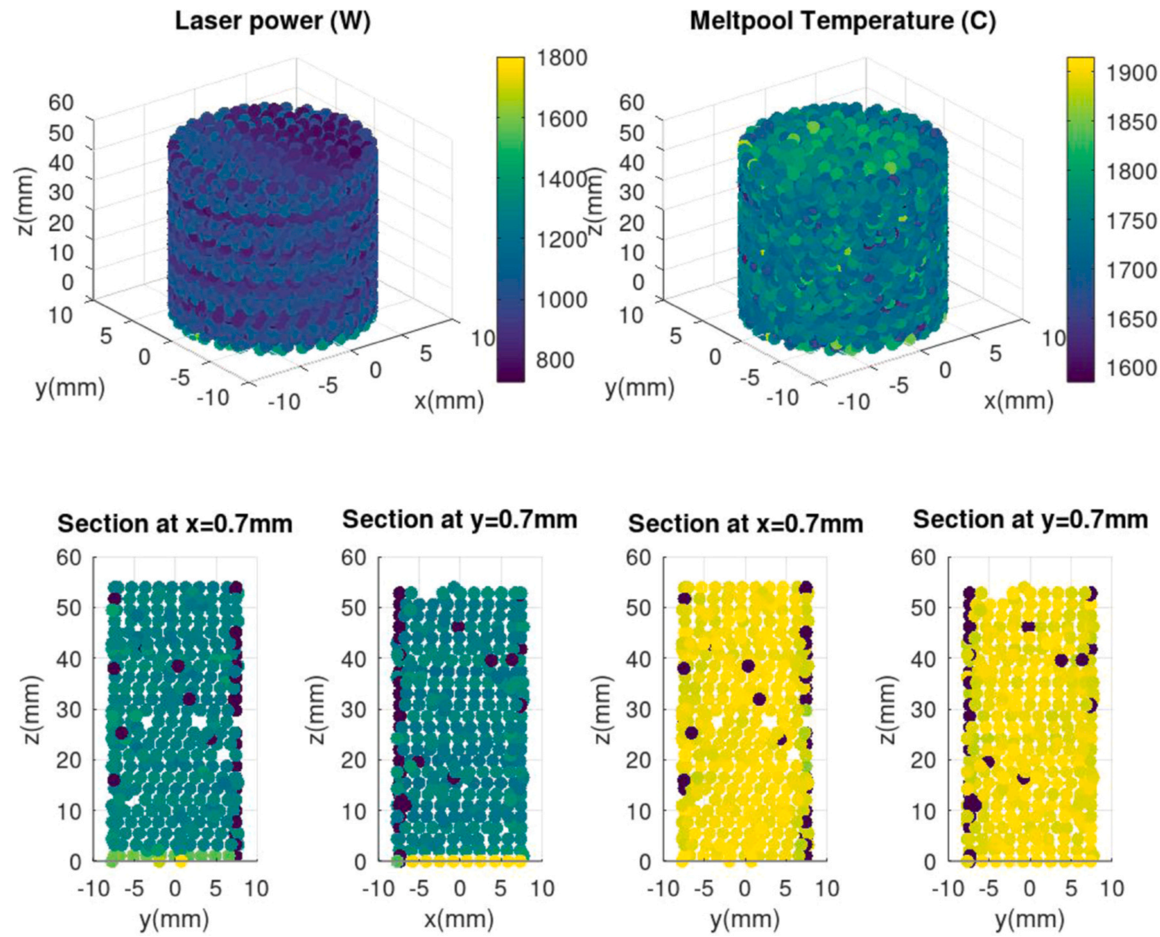


**Fig. 7.** Spatial analysis of the monitored deposition data for one of the type 2 coupons. The laser power setting at each measured location (top left) with two section views bottom left. The evolution of the meltpool temperature (top right) with two section views (bottom right).

order to detect any anomalies with the deposition process. Fig. 7 presents a spatial analysis of the monitored data for one of the type 2 coupons. The left side of the figure presents the laser power setting in each of the measured locations as well as two section views directly below. On the right-hand side, the evolution of the melt pool temperature is presented.

In order to investigate the deposition further and acquire comparable characteristics between each of the deposited coupons, the time domain representation of the data was examined. In Fig. 8 the time-based data for the melt pool size and temperature as well as the laser power are presented. The left side of the figure presents the time domain of the measurements; the observations did not show any measurable characteristic apart from maximum values. By creating the histograms for each measurement, the characteristics of each measured can be observed. The distribution of values for each data stream can be observed on the right side of Fig. 8.

Fig. 9 and Fig. 10 present the distribution of laser power and melt pool temperature values for the samples that were examined in the testing campaign. As it can be observed all six samples present the same distribution shape and magnitude in both the laser power and the melt pool temperature.

Deposited samples were also sectioned polished and etched using standard metallographic techniques in order to investigate potential deposition issues such as porosity, lack of fusion defects and cracks that could be detrimental to the performance of the samples. Fig. 11 and Fig. 12 present micrograph images extracted from an as deposited 15-5PH sample. As it can be observed no defects that would influence the performance or the coupon are present. With very small levels of porosity present, which is common place with AM material [28], with no single pore larger than 50 µm in diameter present in the examined samples.

### *15-5PH Stainless Steel tensile testing*

The results of the tensile testing have been split into three sections. *Type 1: As built vs forged* compares the as-built AM 15-5 PH material against a comparable 15-5PH forged sample. *Type 1: Heat treatment and HIP* compares the performance of different heat treatment strategies for the 15-5 PH AM material. T*ype 2 samples: 50% AM 15-5, 50%17-7* presents the results from the Type 2 samples.

For the Type 1 samples the large nature of the block from which they were extracted results in an increased level of uniformity compared with small structures like thin walls and tower like geometries such as the Type 2 samples, where the relative heat input can be much larger.

### *Type 1: As built Vs forged*

The stability of the deposition process afforded by the large block results in a very low variability of tensile strengths across the repeat samples, as shown by the error bars in Fig. 13. Comparing the 15-5

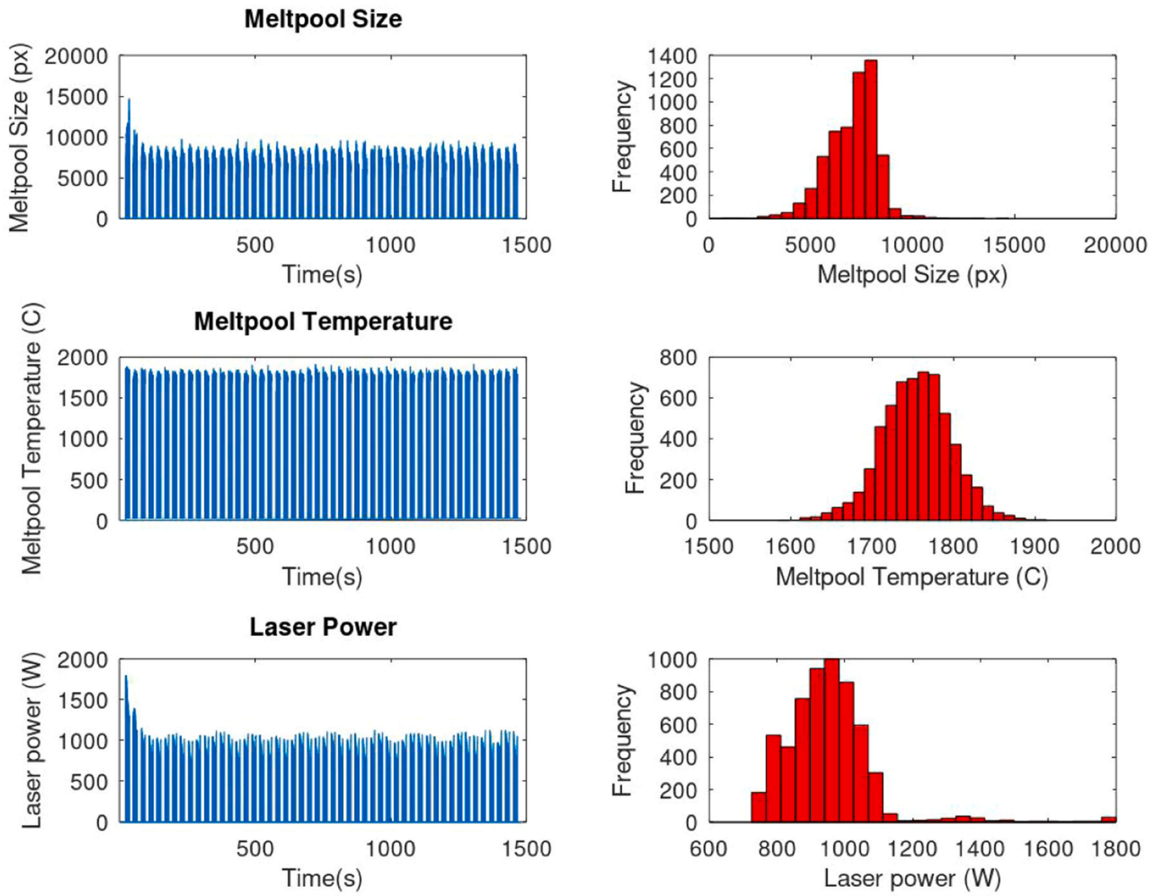


**Fig. 8.** Meltpool size (in pixels), meltpool temperature (in °C) and laser power (in W) during deposition.

PH AM as built data with the forged 15-5 PH samples it can be seen that the AM material has recorded a lower tensile strength in both the longitudinal and transverse orientations. With the AM material on average being 91% the strength of the average forged tensile value.

Looking at the error bars for the elongation of the forged samples it can be seen that they vary more than AM samples which is an interesting finding as it is generally accepted that forged material is more predictable and uniform in nature than AM material. It can also be seen that the forged material had much larger levels of elongation than the AM material. Concentrating on the AM material, the elongation of the longitudinal direction samples were lower than the transverse samples, with a tighter grouping of results. The likely explanation for this lower level of elongation is due to the grain structure of the sample. Commonly in layer AM, material grains can be seen to grow in the direction of the heat source, often multiple layers in length. This orientation of grains results in the transverse tests pulling the sample parallel with the grain direction, as opposed to the longitudinal samples where the material is being pulled perpendicular to the grain direction.

Table 7 shows images of the fractured samples, comparing the transverse and longitudinal 15-5 PH AM as-built samples with the 15-5 PH forged specimen. Here it can be seen that there are noticeable lines of some sort of inclusion. Without precise examination of these regions, it isn't possible to state what these are however, due to the spacing of the discoloured inclusions and with inspection by eye on a microscope it can be seen that they are not due to porosity and are spaced at the height or width of the deposition path. This seems to suggest that it is something that is formed during the deposition of each track, such as oxidation. Which is then covered by the following layer. This was interesting as no evidence of this has been found in polished cross-sections in this or our previous studies or in the machined surface of parts that have been deposited and later machined.

The fracture type for the additive material can be seen to be brittle, with the longitudinal sample appearing to slightly more brittle than the transverse sample. While the forged specimen evidences a much more ductile fracture mechanism, with necking of the fracture zone present.

The 1248 MPa average tensile strength is higher than what is typically reported (1172 MPa), but this is still higher than the average as-built strength of 15-5 PH (1138 MPa), which was the next strongest material [1]. The results demonstrate that the combination of a martensitic microstructure and precipitation hardening is greater than a fully martensitic microstructure, while also having a greater ductility due to having less residual stress than the as-built AM samples [6]. From this explanation, it is possible to understand why forged 15-5PH has higher strength and ductility than as-built 15-5PH.

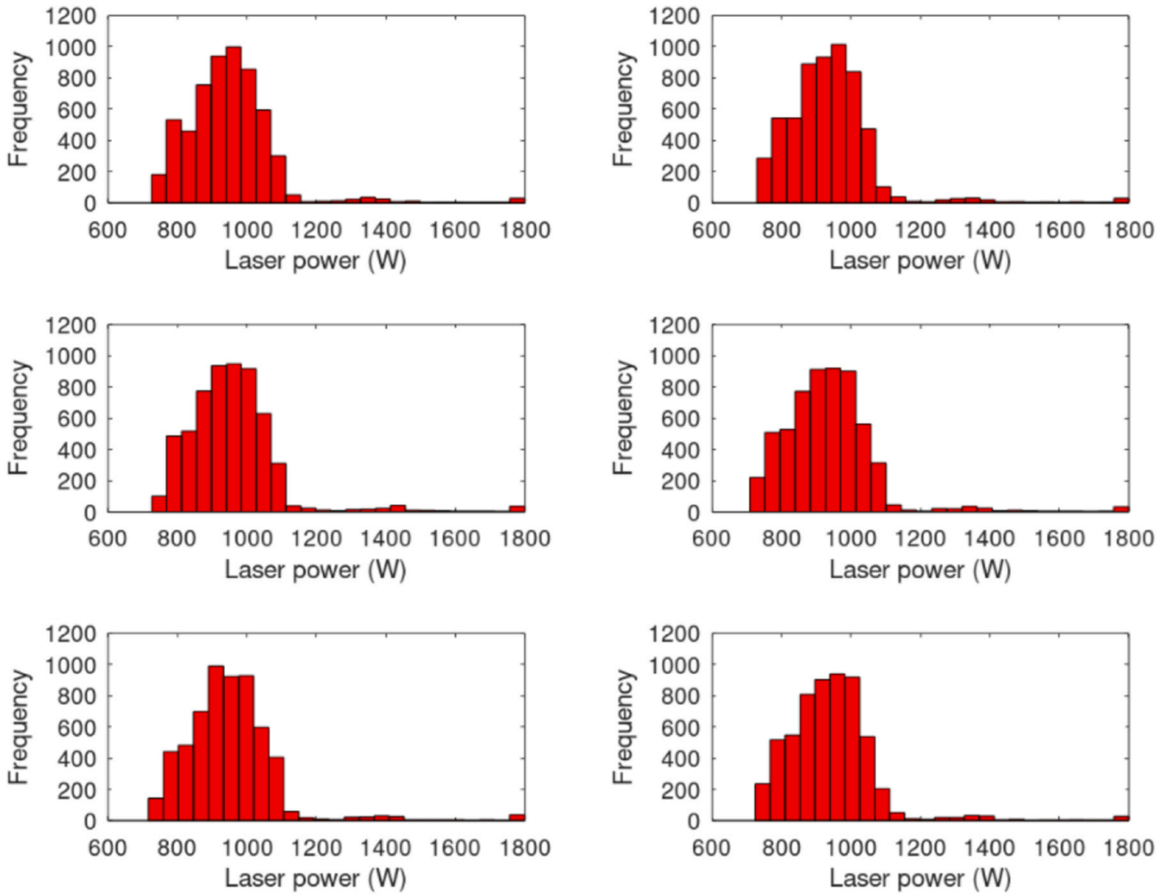


**Fig. 9.** Laser power distribution for the examined samples.

*Type 1: Heat treatment and HIP*

Heat treatment of AM material is still very much a non-perfected art. In this case two types of heat treatments were deployed and compared against each other, and a combination of the two. This is described in more detail in *Experimental procedure*.

The HIP process uses high pressure and temperature to reduce the porosity of parts, Fig. 14 shows that in this case this resulted in improved strength of the material compared to the other heat treatments. However, it is worth noting that this value was still lower than the tensile strength for the as-built AM material. Of the three heat treatment combinations, the H1025 heat treatment resulted in the lowest tensile strength, very slightly lower than that of the combined HIP & H1025 treatment. Comparing the effect of sample orientation, the longitudinal samples were found to have slightly lower levels of tensile strength than the transverse samples for all heat treatment types, and the variation of tensile strength results for each was low.

Regarding elongation the HIP process resulted in much lower values of elongation compared to the other two heat treatment conditions, and was more in line with values seen in the as built AM material. The H1025 heat treatment appeared to bring the average elongation closer to that of the forged material, however it can be seen from the error bars on Fig. 14 that the for the elongation there was a large variation in results. This points to the fact that the heat treatment deployed for the 15-5PH, based on one currently used for cast 15-5PH parts was not suitable and requires refinement. However, in part, this variation was due the effect of the sample orientation. For all heat treatment types the elongation was much larger for the transverse samples than the longitudinal samples (Table 8).

The HIP settings used consisted of heating to 1120 °C and holding at that temperature for 3 h. While there are no microstructure results that can provide confirmation, it is highly likely that substantial grain growth has occurred (due to the temperature being higher than the recrystallisation stop value), while the microstructure will have transformed from martensite into the less strong austenite phase [7]. If any precipitates had formed during AM or during the HIP treatment, they will quickly coarsen in size and not contribute to strengthening the steel or preventing grain growth. The large grain size will reduce the elongation values recorded, which counters the effect of the formation of austenite, which is naturally more ductile than martensite.

The strength and ductility measurements for the heat treated and HIP plus heat treated AM samples are similar to each other, which indicates they share similar material properties. The reason for this is that heat treatment was the final operation for both of these groups of samples, therefore the final microstructure will more closely resemble the effects of the heat treatment. In both cases, the strength values are lower than what has been obtained for the other 15-5 PH steels, and the range of elongation results is very wide. The

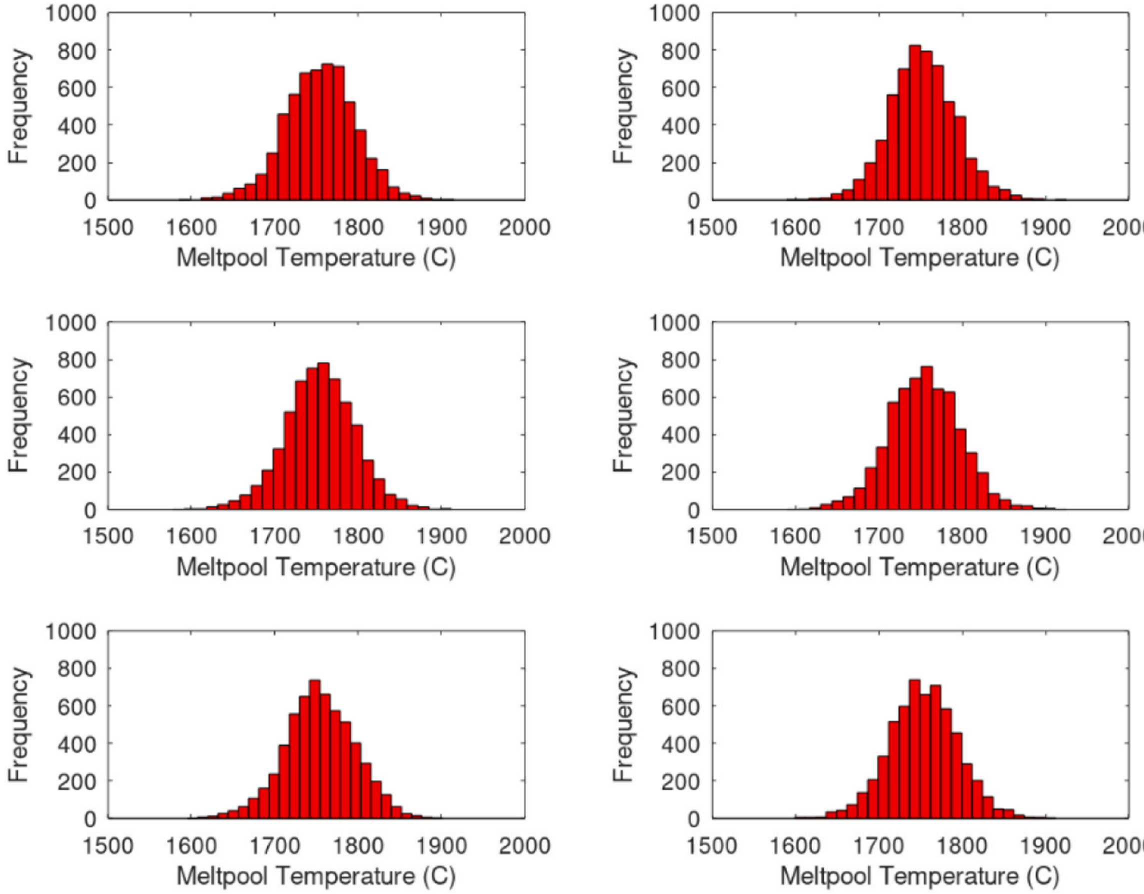


**Fig. 10.** Meltpool temperature distribution for the examined samples.

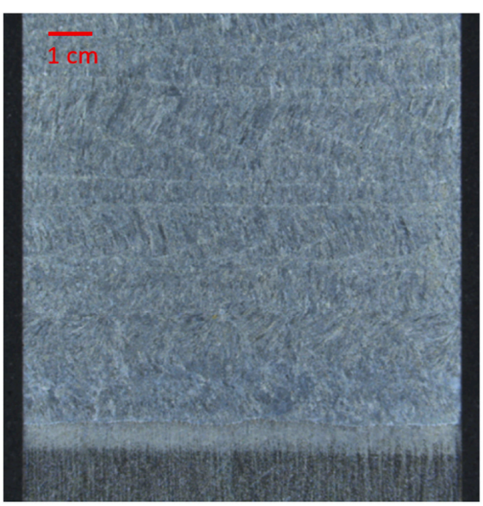


**Fig. 11.** Macro image of a polished and etched sample.

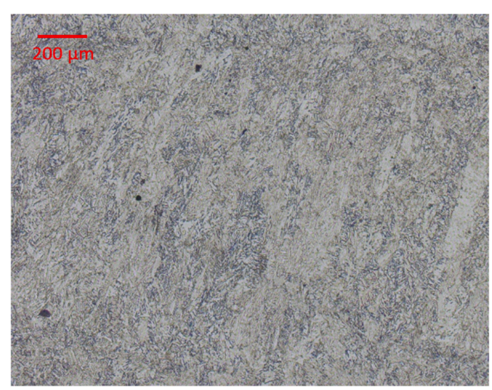


**Fig. 12.** Micro image of a polished and etched sample, showing fine grain structure and small levels of porosity.

wide elongation results indicate that either the microstructure is very heterogeneous, or that there was an issue with consistency when the samples were heat-treated.

Table 9 shows images of fractured samples for each heat treatment strategy. As with the as-built samples dark inclusions appear to be present along the interface of layers, seen in both sample orientations.

The fracture method for these samples was generally very brittle compared with the forged sample seen previously. However, looking at the surfaces of the samples it can be seen that the longitudinal samples had much flatter fracture surfaces, with the transverse samples having sharp areas protruding from the surface, presenting a slightly more mixed fracture method.

*Type 2 samples: 50% AM 15-5, 50%17-7*

This section presents the results from the Type 2 samples, which were created using 50% 15-5 PH AM material and 50% 17-7 PH forged material as described in *Experimental procedure*. This comparison aimed to analyse the performance of the bond between the AM material and its substrate, investigating if any weakness occurred at this boundary.

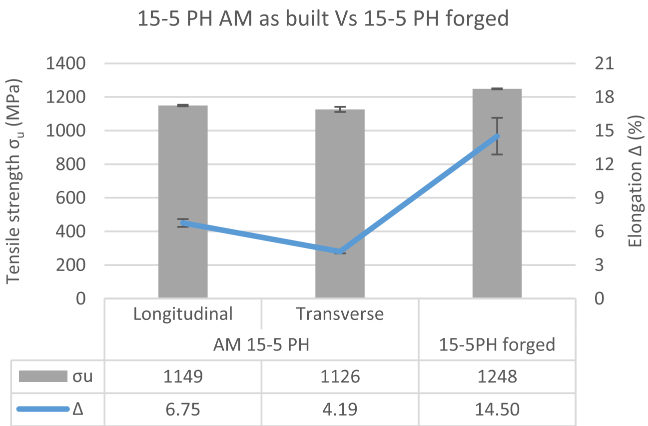


**Fig. 13.** 15-5 PH AM as built (type 1) Vs 15-5 PH forged.

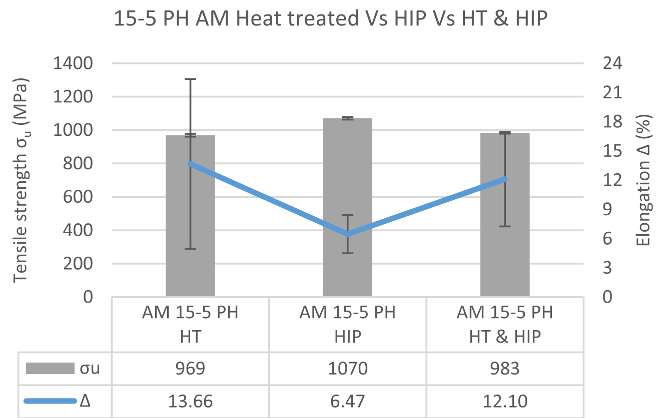


**Fig. 14.** 15-5 PH AM Heat treated Vs HIP Vs HT & HIP.

Fig. 15 shows the results of both forged 15-5 PH and 17-7 PH materials, along with the as-built and heat treated type 2 samples. It can be seen that the 17-7 PH steel produced tensile strength and elongation results (862 MPa, 38.9%) that are comparable with the values found for Condition A 1750 (827 MPa, 45%), which involves heating the steel to 1750 °F (954 °C) and holding for 10 min [8]. This produces an austenite microstructure with no martensite formation or precipitation, making the steel ductile but soft. When 15-5 PH is deposited onto this material (creating 15-5/17-7 as-built) the mechanical properties of 15-5 PH will be the same as 100% as-built 15-5 PH.

Table 10 shows the fracture surfaces of both forged materials and the type 2 samples in each condition. During the tensile testing of 15-5/17-7 as-built samples, the material failed in the forged 17-7 PH region, meaning that the tensile results collected will more closely resemble the mechanical properties of 17-7 PH. The tensile properties of 15-5/17-7 as-built closely resemble that of forged 17-7 PH, with the ductility being reduced and the strength slightly increased.

**Table 7**
Images of fractured surface after tensile test.

| | Transverse | Longitudinal |
|---|---|---|
| 15-5PH AM AB | 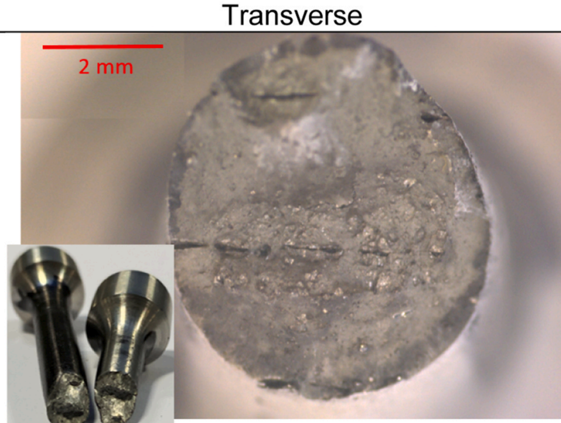 | 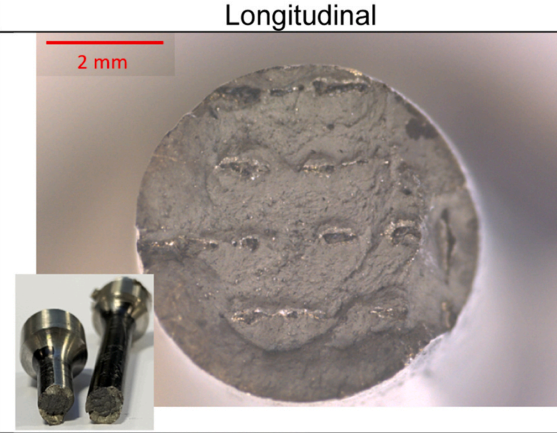 |
| 15-5 PH Forged | 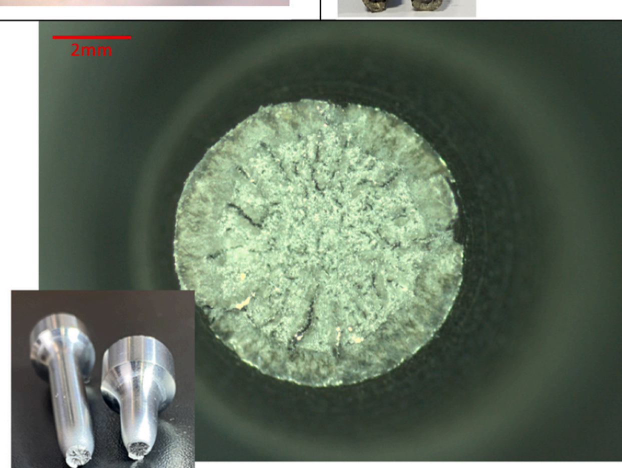 | |

**Table 8**
Comparing sample orientation for 15-5 PH AM Heat treated Vs HIP Vs HT & HIP.

| | AM 15-5 PH HT | | AM 15-5 PH HIP | | AM 15-5 PH HT + HIP | |
|---|---|---|---|---|---|---|
| | Transverse | Longitudinal | Transverse | Longitudinal | Transverse | Longitudinal |
| Tensile Strength (MPa) | 974 | 963 | 1076 | 1064 | 985 | 980 |
| Elongation (%) | 19.60 | 7.72 | 7.92 | 5.01 | 15.19 | 9.01 |

It is predicted that the deposition process heated the 17-7 PH material enough for grain growth to occur, which reduces the ductility. Additionally, the heating and cooling cycles would encourage rapid melting and solidification, which promotes residual stress formation and dislocation generation, resulting in an increase to the strength of the material.

The 15-5/17-7 HT material failed at the additive 15-5 PH region, which means that the tensile properties for these samples will resemble the AM material instead of the forged 17-7 PH. This sample has mechanical properties that closely match the 15-5 PH HT and 15-5 PH HIP plus HT samples, which shows that the heat treatment has a dominating effect on the material properties. The heat treatment

**Table 9**
Images of fractured surface from the tensile coupons for the 15-5PH AM material after heat treatment, HIP and HIP and heat treatment.

| | Transverse | Longitudinal |
|---|---|---|
| 15-5PH AM HT | 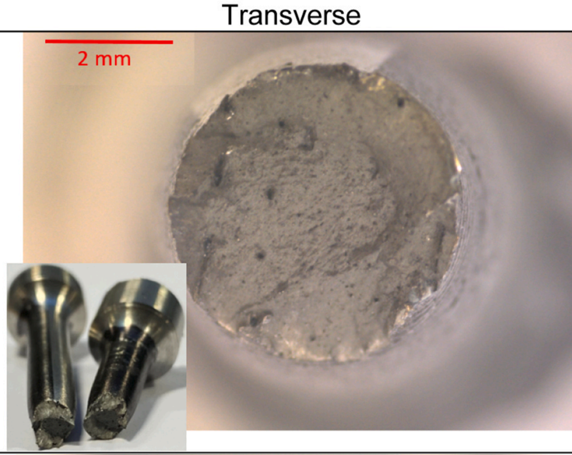  | 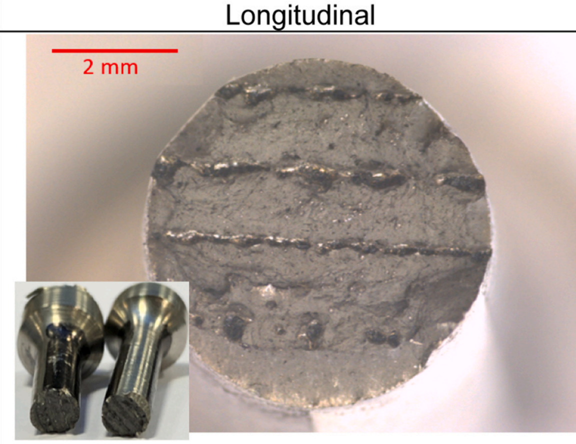  |
| 15-5 PH AM HIP | 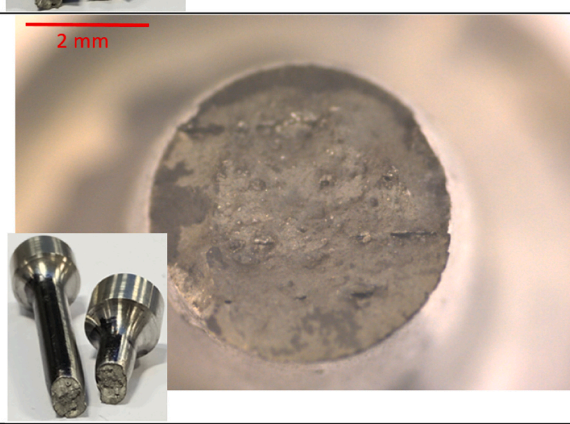  | 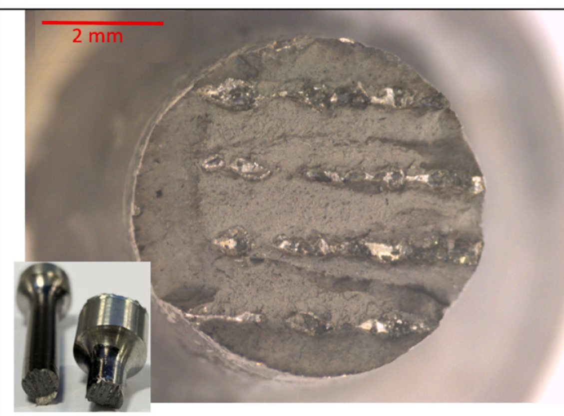  |
| 15-5 PH AM HT & HIP | 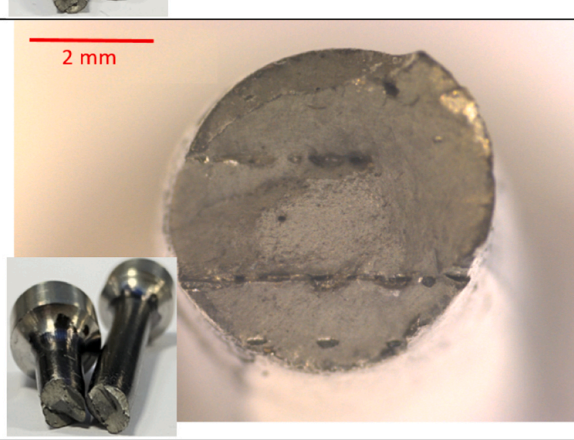  | 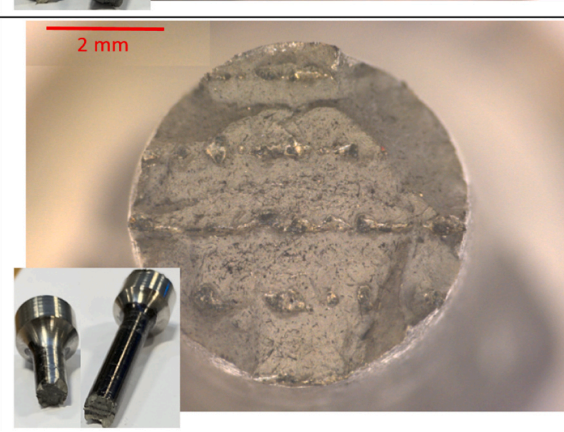  |

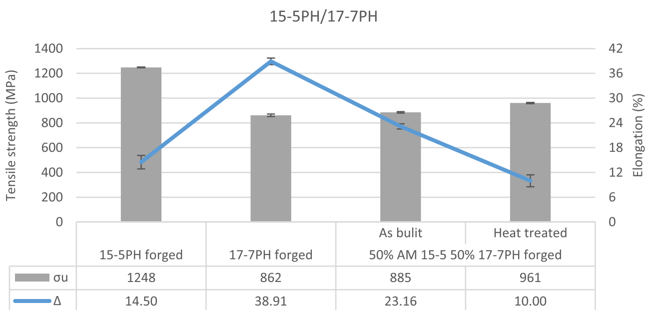


**Fig. 15.** 15-5 PH forged Vs. 17-7 PH forged Vs. 50% AM 15-5, 50%17-7 As built and heat treated.

process on 15-5/17-7 HT has once again produced a 15-5 PH material with relatively low strength and poor ductility, which is why it failed during tensile testing compared with 17-7 PH. This demonstrates that this heat treatment is not an effective method of producing samples with good mechanical properties, and that refinement of the post-processing step is required. Therefore, for the current set-up the as-built material will produce samples that are generally better suited to most engineering roles.

Looking at the fracture mode it can be seen that both forged materials displayed a ductile fracture with necking present. As described the as-built sample fractured in the parent 17-7 material, which has resulted in a very similar fracture to that of the 17-7PH material. While the heat-treated type 2 sample has a cup-and-cone fracture surface, which is more typical of a mixed failure mode.

*Summary*

The as-built 15-5 PH AM material was found on average to be 91% the strength of the average 15-5 PH forged tensile value. Across all AM material conditions the samples taken in the longitudinal direction, as defined by Fig. 3, had a slightly lower tensile strength that of the corresponding transverse sample. As was also the case for the elongation, however this was affected by a large variation across the results, especially in the heat-treated samples.

It was found that samples that had a low elongation before failure (4–10%) underwent primary brittle failure, while samples with high elongation (over 20%) experienced ductile failure. Many samples that failed between 10% and 20% elongation experienced some degree of necking or cup-and-cone fracture surfaces, which is typically found for mixed failure mode.

**Table 10**
Images of fractured surface from the tensile coupons for the forged 15-5PH, forged 17-7PH, type 2 as-built and type 2 after heat treatment.

| 15-5 PH forged | 17-7 PH forged |
|---|---|
| 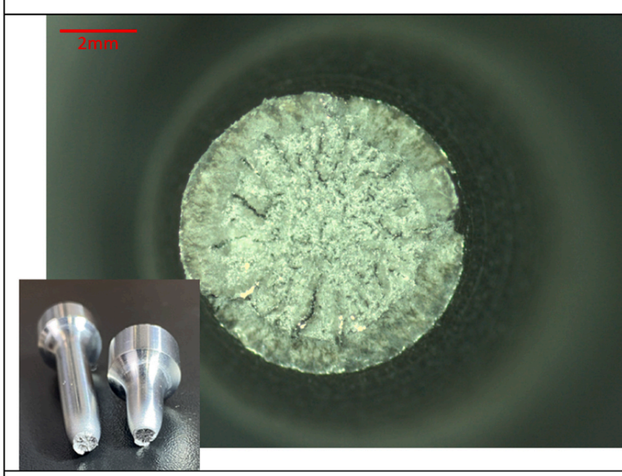 | 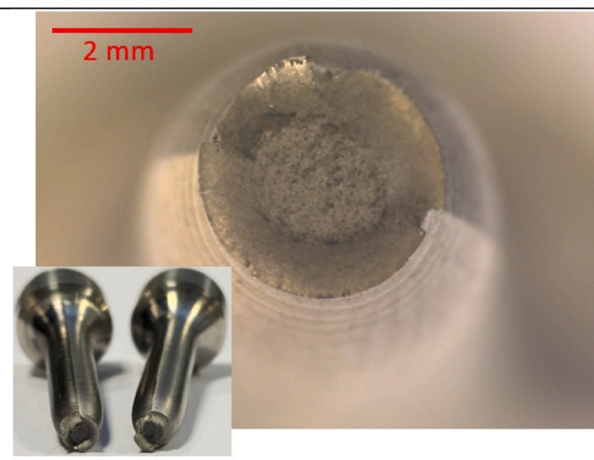 |
| 50% AM 15-5, 50%17-7 Heat treated (H1025) | 50% AM 15-5, 50%17-7 As built |
| 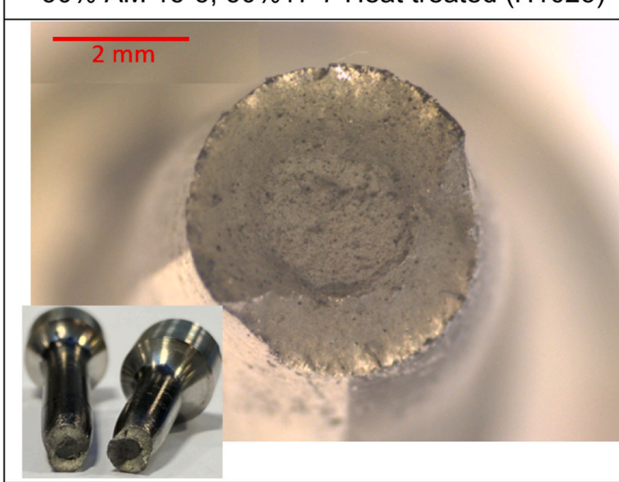 |  |

Another interesting observation is the fracture surface of the heat-treated samples. The tensile results showed a wide range of elongation results, which is translated to the failure mechanism. For example, the failure mode of the heat-treated samples changes within the same sample type, even when the build orientation is the same. This indicates that the modified H1025 heat treatment is producing highly variable microstructures, which results in different failure mechanisms occurring during tensile testing. It is therefore recommended that this heat treatment route is to not be used in the future, unless extensive research is carried out to explain and correct the inconsistent mechanical properties and microstructure. As the HIP procedure creates stronger and more consistent samples compared to the heat-treated samples, the motivation for improving the modified H1025 is low.

## Conclusion

Analysis of the 15-5 PH powder prior to deposition was completed in terms of its particle size distribution (laser diffraction & imaging), powder morphology (imaging and SEM) and flow properties (FT4 and Hall flow). The analysis showed that on the whole the powder was highly spherical, with a relatively low number of satellites. The effects of baking if any on these characteristics were investigated. It was found that the particle size distribution and rheology of the powder was not affected significantly in anyway by the baking procedure. However, the hall flow properties for 15-5PH were affected by the baking (reducing the time slightly and bringing the time closer to the manufacturer's value on the specification sheet).

Deposition was performed using the parameters shown in Table 2. Analysis of the meltpool temperature and laser power during the deposition along with a polished and etched cross-section of the deposited material is shown in *Equipment*. Low levels of porosity and no evidence of cracking was seen in the sectioned material. The data presented in this section showed that the deposition process was very repeatable with almost identical heat histories seen when repeating the processing of identical parts. The thin, tower like nature of the type 2 samples can cause issues with heat management for blown powder DED processes. However, the deposition analysis of these samples showed that the devised method maintained a very level meltpool temperature across the process.

Tensile testing was completed on the 15-5PH AM material in the as built, heat treated, HIP, HIP & heat treated conditions, and also using forged 15-5 PH material for comparison. It was found that in the as-built condition the AM material was 91% the strength of the forged material. Whilst all heat treatments resulted in a decrease in tensile strength, most of all the H1025 heat treatment. For elongation it was found that the heat treatment resulted in much larger variation between repeat results, leading to the conclusion that the H1025 heat treatment was not suitable for the AM material.

Comparisons of sample orientation showed that a slight reduction in tensile strength and the recorded elongation was present when samples were taken in the longitudinal orientation compared to the transverse orientation.

The type 2 tensile samples consisted of 50% 17-7 PH stainless steel and 50% AM 15-5 PH stainless steel, with the interface boundary between the two materials located at the centre of the tensile sample. This test was designed to investigate the quality of the bond between AM material and substrate, specifically when using dissimilar materials. The results of this test showed that the bond was indeed stronger than the surrounding material, with the fracture zone occurring away from the centre of each sample. It was found that for the As-built samples the sample fractured in the weaker 17–7 PH material, while for the heat-treated samples the fracture was in the 15-5 PH AM material. This further validated the conclusion that the H1025 heat treatment currently used for treatment of 15-5 PH cast parts is not suitable for AM material.

## Declaration of Competing Interest

The authors declare that they have no known competing financial interests or personal relationships that could have appeared to influence the work reported in this paper.

## References


[1] AK Steel, "15–5PH Stainless Steel," 12 2018. [Online]. Available: ⟨https://www.aksteel.com/sites/default/files/2018-12/15-5-ph-stainless.pdf⟩.
[2] AK STeel, "17–7 PH Stainless Steel," 01 2018. [Online]. Available: ⟨https://www.aksteel.com/sites/default/files/2018-01/177ph201706.pdf⟩.
[3] Couturier, L., Geuser, F.D., Descoins, M., Deschamps, A., 2016, Evolution of the Microstructure of a 15-5PH Martensitic Stainless Steel During Precipitation Hardening Heat Treatment. Materials & Design, 107:416–425.
[4] Weinberger, T., Enzinger, N., Cerjak, H., 2013, Microstructural and Mechanical Characterisation of Friction Stir Welded 15-5PH Steel. Science and Technology of Welding and Joining, 14/3: 210–215.
[5] Alafaghani, A., Qattawi, A., Castañón, M.A.G., 2018, Effect of Manufacturing Parameters on the Microstructure and Mechanical Properties of Metal Laser Sintering Parts of Precipitate Hardenable Metals. The International Journal of Advanced Manufacturing Technology, 99:2491–2507.
[6] Fakic, B., Cubela, D., 2013, Review of the Development of Research in the Design of Semi Austenitic Stainless Steel 17-7PH. Trends in teh Development of Machinery and Associated Technology. TMT, Istanbul, Turkey.
[7] Xu, X., Yu, Z., 2008, Metallurgical Analysis on a Bending Failed Pump-shaft Made of 17-7PH Precipitation-hardening Stainless Steel. Journal of Materials Processing Technology, 198/1–3: 254–259.
[8] DebRoy, T., Wei, H.L., Zuback, J.S., Mukherjee, T., Elmer, J.W., Milewski, J.O., Beese, A.M., Wilson-Heid, A., De, W.Z.A., 2018, Additive Manufacturing of Metallic Components – Process, Structure and Properties. Materials Science and Engineering, 92:112–224.
[9] Park, J.S., Lee, M.-G., Cho, Y.-J., Sung, J.H., Jeong, M.-S., Lee, S.-K., Choi, Y.-J., Kim, D.H., 2016, Effect of Heat Treatment on the Characteristics of Tool Steel Deposited by the Directed Energy Deposition Process. Metals and Materials International, vol. 22/1: 143–147.
[10] K. Coffy, "Microstructure and Chemistry Evaluation of Direct Metal Laser Sintered 15-5 PH Stainless Steel," University of Central Florida, Florida, 2014.
[11] Rafi, H.K., Starr, T.L., Stucker, B.E., 2013, A Comparison of the Tensile, Fatigue, and Fracture Behavior of Ti–6Al–4V and 15-5 PH Stainless Steel Parts mMade by Selective Laser Melting. The International Journal of Advanced Manufacturing Technology, 69:1299–1309.
[12] Yadollahi, A., Shamsaei, N., Thompson, S.M., Seely, D.W., 2015, Effects of Process Time Interval and Heat Treatment on the Mechanical and Microstructural Properties of Direct Laser Deposited 316L Stainless Steel. Materials Science & Engineering A, 644:171–183.
[13] Guo, P., Huang, B.Z.C., Gao, H., 2017, Study on Microstructure, Mechanical Properties and Machinability of Efficiently Additive Manufactured AISI 316L Stainless Steel by High-power Direct Laser Deposition. Journal of Materials Processing Technology, 240:12–22.
[14] Saboori, A., Gallo, D., Biamino, S., Fino, P., Lombardi, M., 2017, An Overview of Additive Manufacturing of Titanium Components by Directed Energy Deposition: Microstructure and Mechanical Properties. Applied Sciences, 7/883: 1–23.
[15] Kim, D.-K., Woo, W., Kim, E.-Y., Choi, S.-H., 2019, Microstructure and Mechanical Characteristics of Multi-layered Materials Composed of 316L Stainless Steel and Ferritic Steel Produced by Direct Energy Deposition. Journal of Alloys and Compounds, 774:896–907.
[16] Tapoglou, N., Clulow, J., 2020, Investigation of Hybrid Manufacturing of Stainless Steel 316L Components Using Direct Energy Deposition. in: Proceedings of the Institution of Mechanical Engineers, Part B: Journal of Engineering Manufacture:0954405420949360.
[17] Wang, Z., Palmer, T.A., Beese, A.M., 2016, Effect of Processing Parameters on Microstructure and Tensile Properties of Austenitic Stainless Steel 304L Made by Directed Energy Deposition Additive Manufacturing. Acta Materialia, 110:226–235.
[18] Oh, W.J., Lee, W.J., Kim, M.S., Jeon, J.B., Shim, D.S., 2019, Repairing Additive-manufactured 316L Stainless Steel Using Direct Energy Deposition. Optics and Laser Technology, 117:6–17.
[19] Wei, S., Wang, G., Wang, L., Rong, Y., 2018, Characteristics of Microstructure and Stresses and Their Effects on Interfacial Fracture Behavior for Laser-deposited Maraging Steel. Materials and Design, 137:56–67.
[20] Spierings, A., Starr, T., Wegener, K., 2013, Fatigue Performance of Additive Manufactured Metallic Parts. Rapid Prototyping Journal, 19/2.
[21] Alafaghani, A., Qattawi, A., Jaman, M.S., Ablat, M.A., 2019, Microstructure and Mechanical Properties of Direct Metal Laser–sintered 15-5PH Steel with Different Solution Annealing Heat Treatments. The International Journal of Advanced Manufacturing Technology, 105:3499–3520.

[22] Buchanan, C., Matilainen, V., Salminen, A., Gardner, L., 2017, Structural Performance of Additive Manufactured Metallic Material and Cross-sections. Journal of Constructional Steel Research, 136:35–48.
[23] Agius, D., Kourousis, K., Wallbrink, C., Song, T., 2017, Cyclic Plasticity and Microstructure of As-built SLM Ti-6Al-4V: The Effect of Build Orientation. Materials Science and Engineering, 701:85–100.
[24] Mendagaliev, R., Klimova-Korsmik, O., Promakhov, V., Schulz, N., Zhukov, A., Klimenko, V., Olisov, A., 2020, Heat Treatment of Corrosion Resistant Steel for Water Propellers Fabricated by Direct Laser Deposition. Materials, 13:2738.
[25] D. Feldt, P. Hedberg, A. Jarlöv, E. Persson, M. Svensson, F. Vennberg and T. You, “A literature study of powder-based additive manufacturing,” Uppsala universitet, Uppsala, Sweden, 2018.
[26] Dass, A., Moridi, A., 2019, State of the Art in Directed Energy Deposition: From Additive Manufacturing to Materials Design. Coatings, 9/7: 418.
[27] ASTM, “ASTM E8 / E8M - 21 - Standard Test Methods for Tension Testing of Metallic Materials,” [Online]. Available: 〈https://www.astm.org/Standards/E8〉.
[28] Tan, Z.E., Pang, J.H.L., Kaminski, J., Pepin, H., 2019, Characterisation of Porosity, Density, and Microstructure of Directed Energy Deposited Stainless Steel AISI 316L. Additive Manufacturing, 25:286–296.